

Effect of amino acid on the passivation, corrosion and inhibition behavior of aluminum alloy in alkaline medium

S.Kharacha^a, A. Batah^b, M. Belkhaouda^{a,b}, L. Bazzi^a, L. Bammou^{a,b}, R. Salghi^b, O. Jbara^c, A. Tara^c

^a Laboratory of Materials & Environmental, Faculty of Science, Ibn Zohr University, Agadir, Morocco

^b Laboratory of Environmental Engineering and Biotechnology, ENSA, University Ibn Zohr, PO Box 1136, 80000 Agadir, Morocco.

^c Laboratoire d'Analyse des solides Surfaces et Interfaces, UTAP EA 3802, Faculté des Sciences, Université de Reims, UMR 6089, Moulin de la housse, BP :1039, FR-51687 Reims Cedex 2, France;

Abstract

The effect of L-methionine (L-Met) on the passivation and corrosion inhibition of aluminum alloy was investigated in carbonate medium in presence of chloride ions. This inhibitive action against the corrosion of aluminum in corrosive solution was investigated at 298 K using potentiodynamic polarization curves (PDP), cyclic voltammetry (CV) and electrochemical impedance spectroscopy (EIS). The results obtained from the polarization curves reveal that the aluminum in alkaline medium exhibits a phenomenon of passivation with breakdown of passivity. Temperature effect on the corrosion behavior with the addition of (L-Met) studied in the range of temperature from 298 to 328 K. The inhibition efficiency decreases slightly with the increase in the temperature. Results show that L-Met is a good inhibitor and inhibition efficiency reach 87,23% at 10^{-3} M. The electrochemical results are confirmed by scanning electron microscopy (SEM). The adsorption of this compound on aluminum surface obeys Langmuir's adsorption isotherm. The kinetic and thermodynamic parameters were determined and discussed.

* Corresponding author:
m.belkhaouda@uiz.ac.ma

Received 16 Oct 2017,

Revised 23 Jan 2018,

Accepted 24 March 2018

Keywords: Adsorption, Corrosion inhibition, Polarization Curves, cyclic voltammetry, EIS, amino acids, aluminum alloy Empirical

1-Introduction

Aluminum and its alloys are widely used for different applications in the industries and marine environment because of their excellent properties [1-3]. The behavior of aluminum and its alloys in aqueous environments depends on several parameters such as the surface properties of the material, the nature, the temperature, pH and the composition of the aggressive solution [4]. The corrosion resistance of aluminum alloy is the results of their ability to form a natural oxide film on the surface in different media [5-7]. However this oxide film can easily undergo corrosion reactions in chloride solutions [8-9]. The corrosion inhibition of aluminum and its alloys is of tremendous technological importance, due to the increased applications of these materials. Many investigators have studied ways to obtain optimum corrosion protection for aluminum in various media, by either finding new inhibitors or improving the inhibition efficiency [10-12]. The inhibitor efficiency has been attributed to the adsorption of the inhibitor molecules on the metal surface, forming a protective layer. The extent of adsorption of an inhibitor depends on many factors: the nature of the metal, the mode of adsorption of the inhibitor and the surface condition [13-15]. The inhibition effect mainly depends on some physicochemical and electronic properties of the organic inhibitor which relate to its functional groups, steric effects, electronic density of donor atoms, and orbital character of donating electrons [16-19]. Thus, the present work consists to study the inhibitive abilities of L-methionine, named 2-amino-4-(methylthio)butanoic acid, shown in Fig. 1 on the passivation and corrosion of aluminum in Na_2CO_3 0.1 M + NaCl 1M solution using potentiodynamic polarization curves, cyclic voltammetry (CV) and electrochemical impedance spectroscopy (EIS) methods. The surface analysis was carried out using scanning electron microscopy (SEM). The adsorption behavior of the inhibitor was analyzed against Langmuir adsorption isotherm theory.

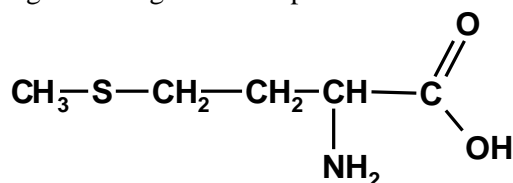


Fig. 1: L-methionine (2-amino-4-(methylthio)butanoic acid)

2-Expérimental procedure

The chemical composition of aluminum alloy is given in Table 1. For potentiodynamic polarization curve, cyclic voltammetry and electrochemical impedance spectroscopy (EIS) techniques, a cylindrical rod embedded in Araldite with an exposed surface area of 0.16 cm^2 .

Table 1: Chemical composition of the aluminum alloy 3003 (AA) used.

Al %	Mg %	Si %	Mn %	Fe %	Zn %	Cu %	Ti %	Ni %	Cr %
Balanced	0.53	0.44	0.04	0.19	<0.002	<0.03	<0.002	<0.003	<0.002

The aggressive solution of Na_2CO_3 0,1M + NaCl 1M were prepared by dilution of Na_2CO_3 and NaCl with bidistilled water. The solution tests are freshly prepared before each experiment. The organic compound tested was the amino acid L-methionine (L-Met). The concentration range of the study of this compound was 10^{-3} to 10^{-6} M.

Impedance measurements are performed at 298K after 1/2 hour of immersion in alkaline medium using VersaSTAT 3 potentiostat and piloted by VersaStudio software under static condition. Electrochemical measurements were performed in a three electrode cylindrical glass cell. The platinum electrode and a saturated calomel electrode (SCE) were used as auxiliary and reference electrodes, respectively. All potentials given in this study were referred to SCE

reference electrode. The working electrode was immersed in test solution for 30 minutes to establish a steady state open circuit potential (E_{ocp}). After measuring the E_{ocp} , the electrochemical measurements were carried out. All electrochemical tests have been performed in aerated solutions at pH=11. The EIS experiments were conducted in the frequency range with high limit of 10 kHz and different low limit 0.1 Hz at open circuit potential, with 10 points per decade, at the rest potential, after 30 min of alkaline immersion, by applying 10 mV ac voltage peak-to-peak. Nyquist plots were made from these experiments and the impedance plots are given in the Nyquist representation. Experiments are repeated three times to ensure the reproducibility. In this study the electrochemical behavior of aluminum alloy electrode in inhibited and uninhibited solution was studied by check in anodic and cathodic potentiodynamic polarization curves. Measurements were carried out in the Na_2CO_3 0,1M+NaCl 1M solution containing different concentrations of the studied inhibitor by changing the electrode potential from -1800 mV to 0 mV versus corrosion potential at a scan rate of 1 mV.s^{-1} . The linear Tafel segments of cathodic curves were extrapolated to corrosion potential to obtain corrosion current densities (I_{corr}). The surface analysis was carried out using scanning electron microscope (SEM). The adsorption behavior of the inhibitor was analyzed against Langmuir adsorption isotherm theory.

3-Results and discussion:

3.1. OCP Measurement

Prior to each polarization or EIS experiment, the working electrodes were immersed in Na_2CO_3 0,1M+NaCl 1M solution for 30min to access the free corrosion potential or the quasi-stationary E_{ocp} value. The plots of E_{ocp} vs time of AA3003 in the absence and presence of inhibitor for 30min are given in Figure 2. We note that the value of open circuit potential moves towards cathodic values.

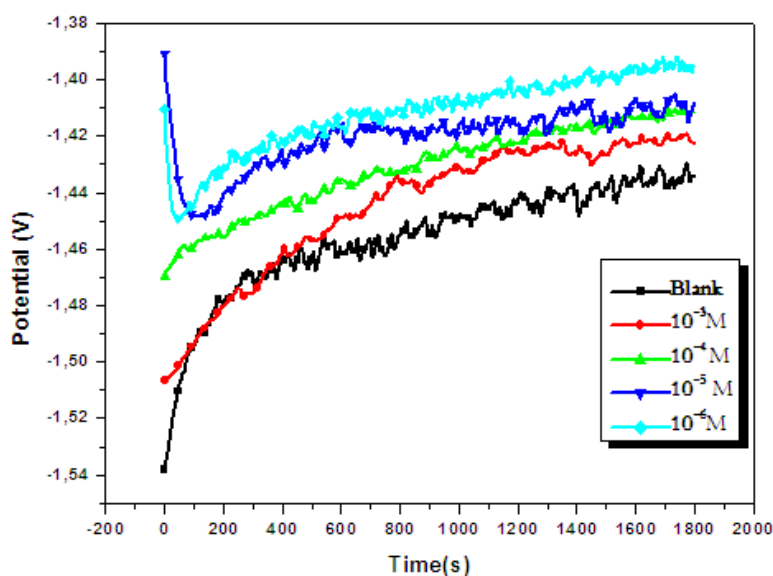


Figure.2: OCP plots for aluminum alloy in Na_2CO_3 0,1M+NaCl 1M containing different concentration of L-Met.

3.2 Potentiodynamic Polarization Curves

Figure 3 show the anodic and cathodic polarization curves for aluminum alloy in Na_2CO_3 0,1M+NaCl 1M at different concentrations of the L-Met inhibitor. In cathodic domain, Tafel behaviour characterised by linear regions in the proximity of the potential of corrosion, indicates that the process of reduction of the water is an activation control [12-13]:



The anodic domain exhibits the permanent passive region and transpassive region. When the surface is covered with passive layer, the anodic current density falls to the lowest value named passive current density I_{pass} representing a permanent passivation. This current density remains almost constant. For more raised anodic potentials, the domain of transpassivity is attained. When the I_{pass} rise suddenly the pitting potential E_{pit} is outrun denoting layer breakdown and we assistant at pitting corrosion phenomenon.

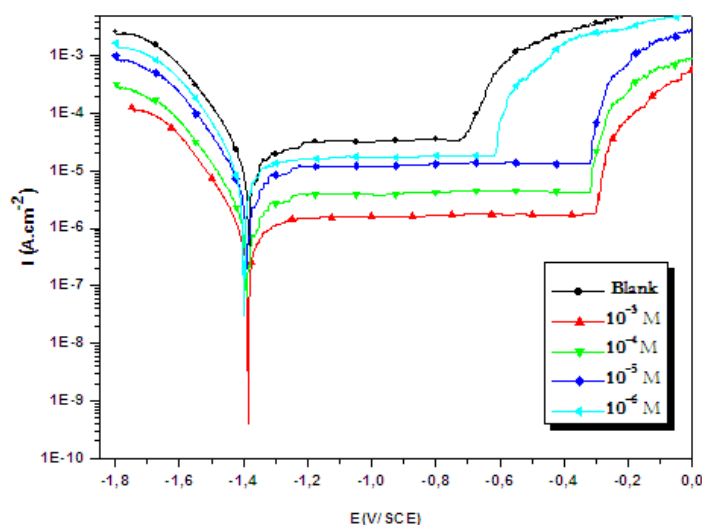


Fig. 3: Polarization curves for aluminum in Na_2CO_3 0,1M+NaCl 1M solution in the presence and absence L-Met at 298K.

It's clear from this figure that the addition of the inhibitor concentration causes a significant decrease in the corrosion rate, a displacement of the anodic curves to more positive potentials and the cathodic curves to more negative potentials. This indicates that L-Met can be classified as mixed-type inhibitor and the molecules containing in tested inhibitor are adsorbed on the cathodic and anodic sites on the electrode surface. The inhibition efficiency values E_I (%), were calculated using the following equation (2).

$$E_I \% = \frac{I_{\text{corr}} - I'_{\text{corr}}}{I_{\text{corr}}} \times 100 \quad (2)$$

Where I_{corr} and I'_{corr} are uninhibited and inhibited corrosion current densities, respectively. Values of the corrosion current densities (I_{corr}), corrosion potential (E_{corr}), cathodic Tafel slope (β_c), passivation current I_{pass} and pitting potential E_{pit} , were determined from Figure 3 and are listed in Table 2.

Table 2: Polarization parameters of aluminum alloy in Na_2CO_3 0,1M+NaCl 1M at 298 K in the absence and presence of L-Met.

Inhibitor	Conc (M)	$-E_{\text{corr}}$ (mV/SCE)	I_{pass} ($\mu\text{A cm}^{-2}$)	$-E_{\text{pit}}$ (mV/SCE)	$-\beta_c$ (mV dec ⁻¹)	I_{corr} ($\mu\text{A cm}^{-2}$)	E_I (%)
Blank	0	1379	34	725	133	142	-
L-Met	10^{-3}	1375	2	296	149	19	86.62
	10^{-4}	1387	4	320	165	28	80.28
	10^{-5}	1382	13	314	159	32	77.46
	10^{-6}	1395	17	615	167	47	66.90

The results from Figure 3 and Table 2 indicate that the corrosion potential is more negative and the corrosion current density (I_{corr}) decreases in the presence of the inhibitor compared to the blank solution and also with increasing the inhibitor concentration which suggest that the presence of this compound retards the dissolution of aluminum electrodes in Na_2CO_3 0,1M+NaCl 1M solution. This implies that L-Met affected both the anodic dissolution of aluminum electrodes and its cathodic reduction, indicating that the L-Met compound could be classified as a mixed-type inhibitor. This can be due to the adsorption of the inhibitor over the corroding surface [20]. We remark also from fig. 3 and table 2 a reduction in the pitting sensitivity that is characterized by the rise in the difference ΔE between the pitting potential and the corrosion potential. The results obtained show that the addition of inhibitor have a considerable effect on the passivation of studied aluminum alloy, in fact, the density of current of passivation decrease with L-Met concentration, reaches a minimum value of $2\mu\text{A cm}^{-2}$ at 10^{-3}M and lead to excellent inhibitive performance.

3.3 cyclic voltammetry measurements

Cyclic voltammetry technic was performed in the solution in the absence and presence of the inhibitor, with the potential (E) swept linearly from -1.8 V/SCE to +0 V/SCE at a sweep rate of 1mV.s^{-1} . Fig. 4 illustrates the cyclic voltammograms curves at various concentrations of inhibitor.

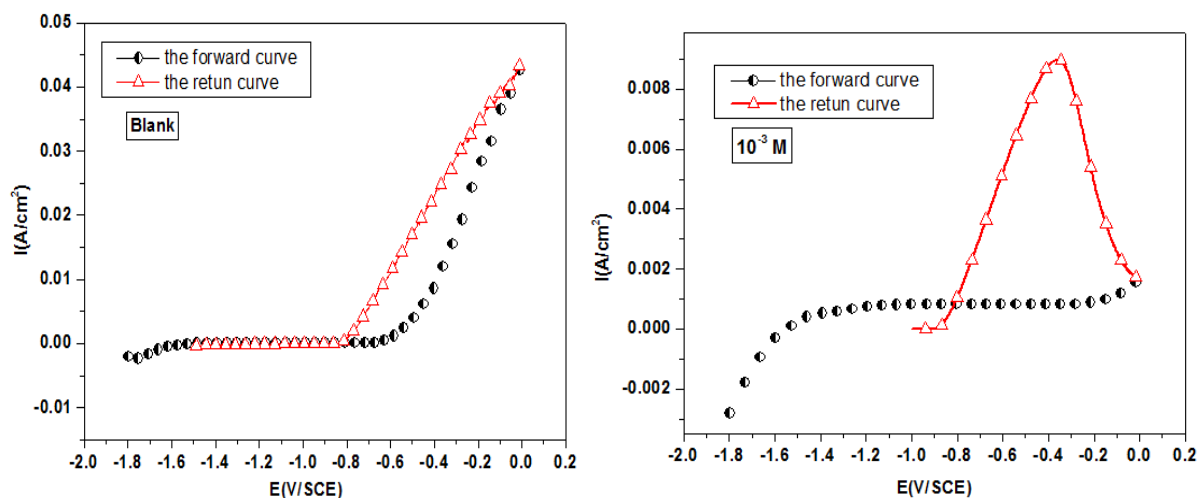


Fig.4: Cyclic voltammetry curves for aluminum electrode in Na_2CO_3 0,1M+NaCl 1M solution in the presence and absence of L-Met at pH=11 and T=298K

The aluminum alloy presents a passivation phenomenon with a breakdown of passivity (Fig.4) in the absence and presence of L-Met inhibitor. It is clear from Figs. 3 & 4 that the pitting potential E_{pit} is modified by addition of the concentration of the inhibitor; in fact, this addition causes a displacement of E_{pit} towards the noblest values and the passive current density I_{pass} decreases with increasing inhibitor concentration.

3.4 Electrochemical Impedance Spectroscopy measurements

The impedance measurements were carried out at room temperature after 30 min of immersion in Na_2CO_3 0,1M+NaCl 1M solution in the absence and presence of different concentration of the L-Met inhibitor. The Nyquist plots for aluminum alloy obtained at the electrode/solution interface without and with L-Met inhibitor are given in Figure 5. Fig 5 show the Nyquist plots present capacitive loops as a depressed semicircle, the diameter of the capacitive loop in

the presence of inhibitor is larger than that in the absence of inhibitor and increases with the inhibitor concentration, indicating that the corrosion is primarily a charge transfer process and the formed inhibitive layer increases by the addition of the L-Met inhibitor [22]. The impedance data are presented in Table 3.

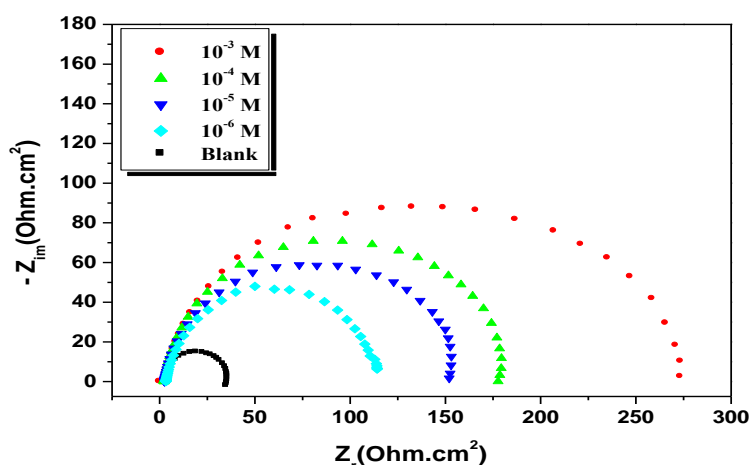


Fig. 5: Nyquist plots for aluminum alloy in Na_2CO_3 0.1M + NaCl 1M containing different concentration of L-Met.

The charge transfer resistance (R_{ct}) values are calculated from the difference in impedance at lower and higher frequencies as suggested by Tsuru et al [21]. The double layer capacitance (C_{dl}) and the frequency at which the imaginary component of the impedance is maximal ($-Z_{\max}$) are found as represented in equation 3:

$$C_{dl} = \frac{1}{2\pi f_{\max} R_{ct}} \quad (3)$$

With C_{dl} : double layer capacitance ($\mu\text{F} \cdot \text{cm}^{-2}$) and f_{\max} : maximum frequency (Hz) The percent inhibition efficiency is calculated by charge transfer resistance obtained from Nyquist plots as follow [23]:

$$E_{R_{ct}} \% = \frac{(R'_{ct} - R_{ct})}{R'_{ct}} \times 100 \quad (4)$$

Where R_{ct} and R'_{ct} are the charge transfer resistance values without and with inhibitor, respectively. It is clear that, the corrosion of aluminum alloy in Na_2CO_3 0.1M + NaCl 1M is clearly inhibited in the presence of the L-Met compound, and the impedance response change with the increase in inhibitor concentration. The quantitative analysis of electrochemical impedance (EIS) spectra was studied on the basis of a physical model characterizing the charge transfer process at the electrode/solution interface. The equivalent circuit as depicted in Figure 6 describes the metal / electrolyte interface of the present corroding system was used to simulate the impedance data (Figure 7).

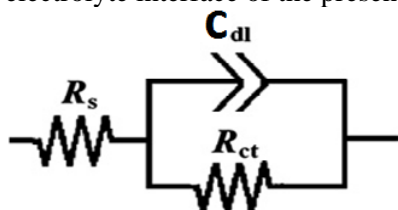


Fig. 6: Equivalent electrical circuit corresponding to the corrosion process on aluminum alloy in Na_2CO_3 0.1M + NaCl 1M

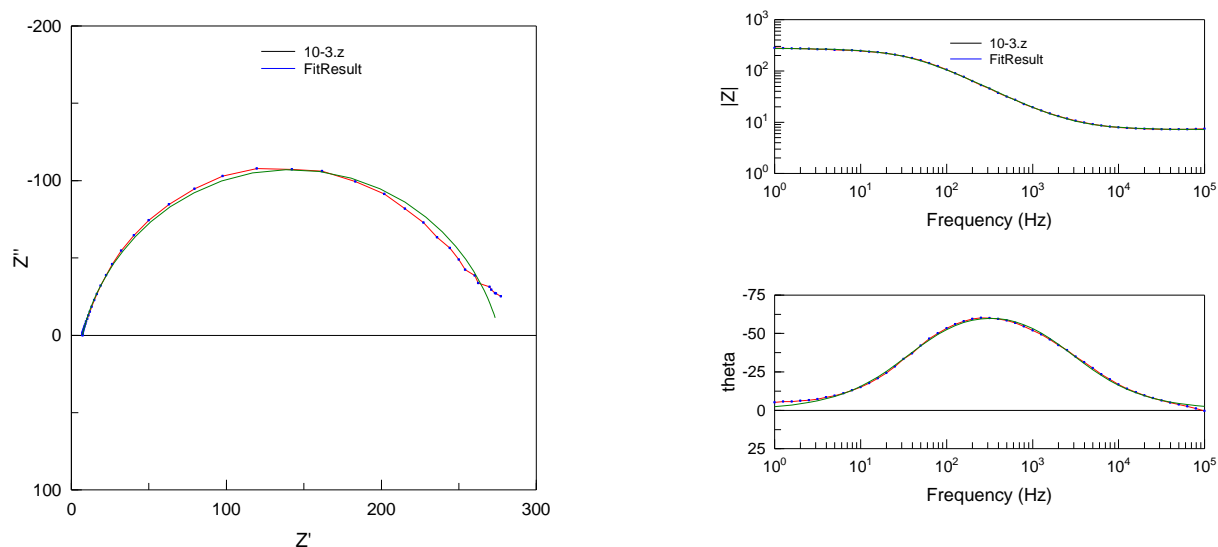


Fig. 7: :EIS Nyquist and Bode plots for AA in Na_2CO_3 0,1M+NaCl 1M of L-Met

Table 3. Electrochemical Impedance for corrosion of aluminum alloy in Na_2CO_3 0,1M+NaCl 1M at various concentration of L-Met.

Inhibitor	C (mol.L ⁻¹)	$R_s(\Omega.\text{cm}^2)$	$R_{ct}(\Omega.\text{cm}^2)$	$C_{dl}(\mu\text{F}/\text{cm}^2)$	E_{Rct} (%)
Blank	0	2,43	35	101	---
L-Met	10^{-3}	2,84	274	29.05	87.23
	10^{-4}	4,15	180	35.38	80.56
	10^{-5}	2,17	156	51.04	77.56
	10^{-6}	5,47	114	55.87	69.30

From the Table 3, the maximum percentage of inhibition efficiency (E_{Rct} %) was achieved at the concentration of 10^{-3} M (87.23%). In the presence of the L-Met the values of R_{ct} has enhanced and the values of double layer capacitance C_{dl} are also brought down to the maximum extent with the increasing of the inhibitor concentration. The decrease in C_{dl} shows that the adsorption of the inhibitors takes place on the metal surface in Na_2CO_3 0,1M+NaCl 1M solution; which can result from a decrease in local dielectric constant and/or an increase in the thickness of the electric double layer [23].

Adsorption isotherm and thermodynamic parameters

It is well recognized that the first step in inhibition of metallic corrosion is the adsorption of organic inhibitor molecules at the electrode/solution interface and that the adsorption depends on the molecules chemical composition, the temperature and the electrochemical potential at the metal/solution interface. In fact, the solvent H_2O molecules could also adsorb at metal/solution interface. So the adsorption of organic inhibitor molecules from the aqueous solution can be regarded as a quasi-substitution process between the organic compounds in the aqueous phase [$\text{Org}_{(sol)}$] and water molecules at the electrode surface [$\text{H}_2\text{O}_{(ads)}$] [24]:



Where (n) is the size ratio, that is, the number of water molecules replaced by one organic inhibitor. Basic information on the interaction between the inhibitor and the steel surface can be provided by the adsorption isotherm. In order to obtain the isotherm, the linear relation between degree of surface coverage (θ) values ($\theta = E_{Rct}\% / 100$) and inhibitor concentration (C_{inh}) must be found. Attempts were made to fit the θ values to various isotherms including Langmuir, Temkin and Freundlich (Figures 8, 9 & 10). By far the best fit is obtained with the Langmuir isotherm. This model has also been used for other inhibitor systems [25, 26]. According to this isotherm, θ is related to C_{inh} by:

$$\frac{C_{inh}}{\theta} = \frac{1}{K_{ads}} + C_{inh} \quad (6)$$

Where θ is the surface coverage, K_{ads} is the adsorption-desorption equilibrium constant, C_{inh} is the concentration of inhibitor. Figure 8 shows the plots of C_{inh} / θ versus C_{inh} and the expected linear relationship is obtained for this compound. The strong correlation ($R^2 = 0.9999$ for the compound L-Met) confirms the validity of this approach. The thermodynamic parameters from the Langmuir adsorption isotherm are listed in Table 4, together with the value of the Gibbs free energy of adsorption ΔG_{ads}^0 calculated from the equation:

$$\Delta G_{ads}^0 = -RT \ln(55.5 \times K_{ads}) \quad (7)$$

Where 55.5 is the concentration of water, R ($8.314 \text{ J} \cdot \text{K}^{-1} \cdot \text{mol}^{-1}$) is the universal gas constant and T is the absolute temperature (K), K_{ads} the adsorption-desorption equilibrium constant [27].

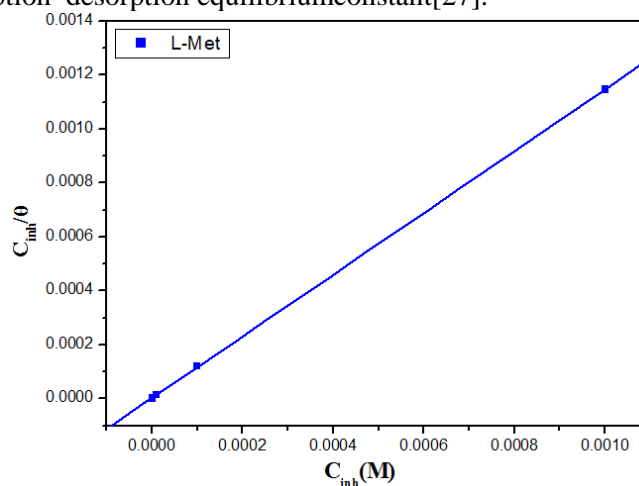


Fig. 8: Langmuir adsorption of inhibitor on the aluminum surface in 0.1 M Na_2CO_3 + NaCl 1M solution at 298K.

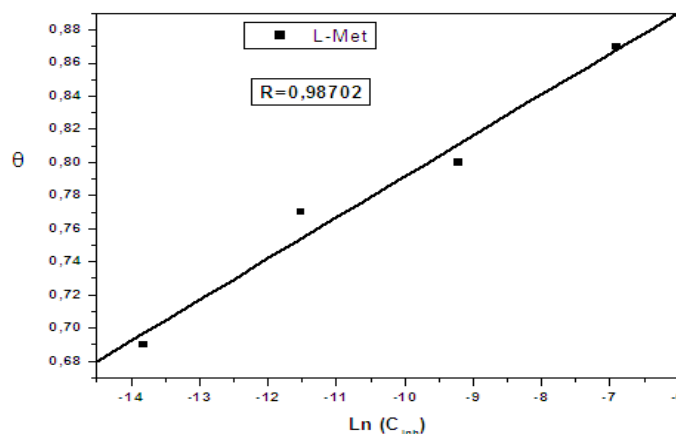


Fig. 9: Plot of Temkin adsorption isotherm

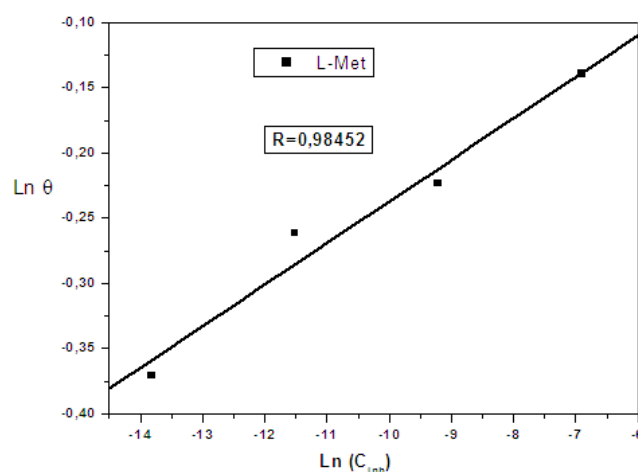


Fig. 10: Plot of Freundlich adsorption isotherm

Table 4: Adsorption parameters of inhibitor for aluminum in 0.1 M Na₂CO₃+NaCl 1M solution at 298K.

Inhibitor	Slope	K _{ads} (M ⁻¹)	R ²	ΔG _{ads} ^o (kJ/mol)
L-Met	1.1444	424872.0073	0.9999	-42.04

In general, energy values of -20 kJ mol⁻¹ or less negative are associated with an electrostatic interaction between the charged molecules and the charged metal surface, physisorption; Those of -40 kJ mol⁻¹ or more negative involve the sharing or transfer of charge of the inhibitory molecules to the metal surface to form a coordinated covalent bond, chemisorption [28, 29]. The standard adsorption free energy value shown in Table 4 suggests that adsorption is chemisorption.

3.5. Effect of temperature

In order to study the effect of temperature on corrosion inhibition of aluminum and to determine the activation energy of the corrosion process, the EIS measurements were obtained at different temperatures in the absence and presence of L-Met in the range of temperature 298-328 K at optimal concentration are given in Figure11. These parameters are useful in interpreting the type of adsorption by the inhibitor. EIS measurements parameters are listed in the Table 5.

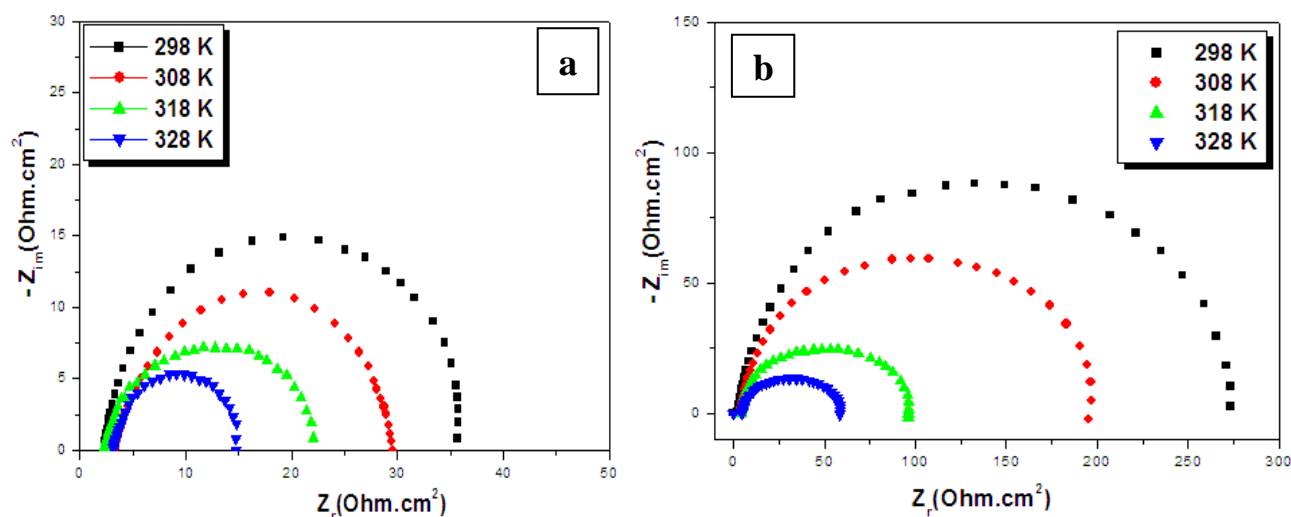


Fig. 11: Nyquist plots for corrosion aluminum 0.1 M Na₂CO₃+NaCl 1M at different temperature (a) and 10⁻³M of L-Met(b).

Table 5.Effect of temperature on the aluminum corrosion in 0.1 M Na₂CO₃+NaCl 1M and at 10⁻³ M of L-Met

Inhibitor	Temp (K)	R _{ct} (Ω.cm ²)	C _{dl} (μF /cm ²)	E _{Rct} (%)
Blank	298	35	101	-
	308	28	56.86	-
	318	22	48.25	-
	328	14	37.91	-
L-Met	298	274	29.06	87.23
	308	195	32.67	85.64
	318	97	41.04	77.32
	328	57	55.87	75.44

The various corrosion parameters obtained are listed in Table 5. The data obtained suggest that L-Met get adsorbed on the aluminum alloys surface at all temperatures studied. Inspection of Table 5 showed that, the temperature rise leads to a decrease of R_{ct} values. Also, the inhibition efficiency of L-Met decreases slightly with the increase in temperature. Values of R_{ct} were employed to calculate values of the corrosion current density (I_{corr}) at various temperatures in absence and presence of L-Met using the following equation [30]:

$$I_{cor} = R T (z . F . R_{ct})^{-1} \quad (8)$$

Where R is the universal gas constant (R = 8.31 J K⁻¹mol⁻¹), T is the absolute temperature, z is the valence of Aluminum (z = 3), F is the Faraday constant (F = 96485 coulomb) and R_{ct} is the charge transfer resistance.

As the corrosion rate is inversely proportional to R_{ct} values of Ln (I_{corr}) and Ln (I_{corr}/T) were plotted as a function of temperature (Arrhenius plots) in Figures 12 and 13 for the corrosion of aluminum in 0.1 M Na₂CO₃+NaCl 1M solutions. The values of E_a, ΔH_a and ΔS_a were estimated from the slopes of the straight lines and given in Table 6.

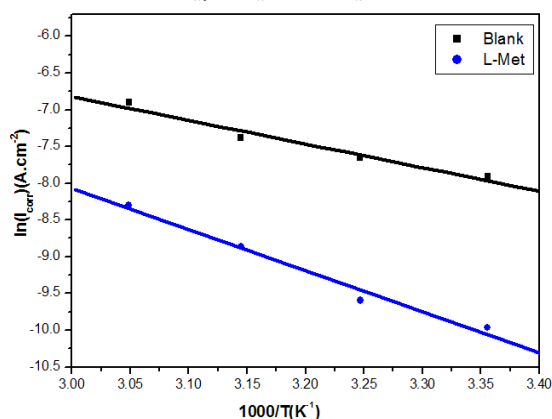


Fig 12: Arrhenius plots of aluminum corrosion in 0.1 M Na₂CO₃+NaCl 1M with and without inhibitor (10⁻³ M)

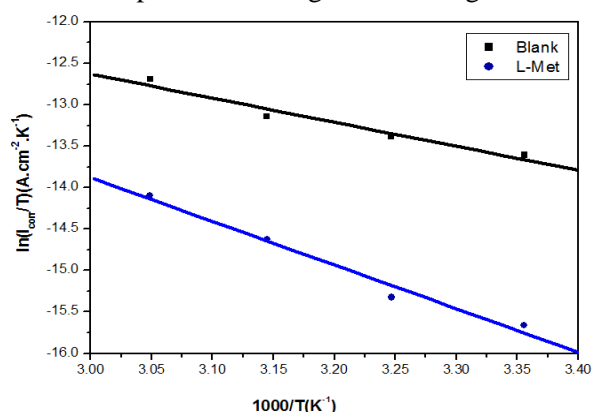


Fig 13: Relation between Ln (I_{corr}/T) and 1000/T at different temperatures (10⁻³ M).

Inspection of Table 6 shows that the value of E_a determined in solution containing (L-Met) is higher than that of in the absence of inhibitor (blank). It revealed an increase of E_a values in presence of inhibitor. For inhibitor, E_a(inhibited solution) > E_a (uninhibited solution), which further confirm E_{Rct}(%) decreases with increase in temperature. A

corresponding increase in the corrosion rate occurs because of the greater area of metal that is consequently exposed to the alkaline environment [31]. On the other hand, the inspection of the same table revealed that the thermodynamic parameters (ΔS_a and ΔH_a) for dissolution reaction of aluminum in 0.1 M $\text{Na}_2\text{CO}_3 + \text{NaCl}$ 1M in the presence of inhibitor are lower than that obtained in the absence of inhibitor. The positive sign of ΔH_a reflects the endothermic nature of the aluminum dissolution process suggesting that the dissolution of aluminum is slow [32]. In the presence of (L-Met), the increase of ΔS_a reveals that an increase in disordering takes place on going from reactants to the activated complex [33].

Table 6. The value of activation parameters E_a , ΔH_a and ΔS_a for aluminum in 0.1 M $\text{Na}_2\text{CO}_3 + \text{NaCl}$ 1M in the absence and presence of L-Met at 10^{-3} M.

Inhibitor	ΔH_a (kJ/mol)	ΔS_a (J/mol)	E_a (kJ/mol)	$E_a - \Delta H_a$
Blank	24.15	-229.93	26.75	2.60
L-Met	43.80	-181.38	46.40	2.60

The difference of the two values is almost constant with an average value of 2.60 kJ.mol^{-1} which is very close to the average value of the product (RT) in the investigated temperature range. Such behavior is characteristic of a unimolecular gas-phase reaction obeying the following equation: [34]

$$E_a - \Delta H_a = RT \quad (9)$$

3.6. Scanning Electron Microscope (SEM).

The surface morphology of aluminum was achieved using Scanning Electron Microscopy (SEM) after 72 hours immersion in 0.1 M $\text{Na}_2\text{CO}_3 + \text{NaCl}$ 1M before and after addition of the L-Met inhibitor. Fig. 14(a) give the micrograph obtained of polished aluminum without being exposed to the corrosive solution. SEM image of aluminum surface after immersion in 0.1 M $\text{Na}_2\text{CO}_3 + \text{NaCl}$ 1M with 10^{-3} M of L-Met is shown in Fig. 14(c). an adsorbed layer on the aluminum surface was created that was observed in Fig. 14(b).

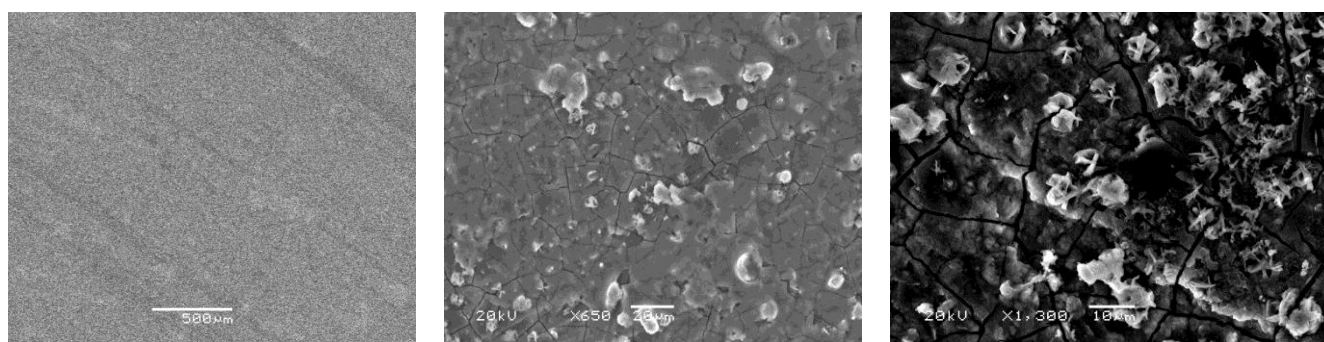


Fig. 14: SEM micrographs of AA surface (a) , AA in 0.1 M $\text{Na}_2\text{CO}_3 + \text{NaCl}$ 1M solution in absence (b) and presence (c) of 10^{-3} M L-Met at 298 K.

4- Conclusion

From the general experimental results the following conclusions can be deduced:

- The L-methionine (L-Met) are found to be a good inhibitor for the corrosion of aluminum in 0.1 M $\text{Na}_2\text{CO}_3 + \text{NaCl}$ 1M and the inhibition efficiency increases with increasing of the L-Met concentration. The E (%) determined by Tafel polarization and EIS methods are in good agreement.
- The polarization curves study show that L-Met compound can be classified as mixed inhibitor. The calculated electrochemical parameters show that the addition of inhibitor L-Met reduces the capacitance C_{dl} values and increase the R_{ct} . It is suggested to attribute this to the increase of the thickness of the adsorption film at steel surface.
- The inhibition is accomplished by adsorption of L-Met molecules on the aluminum surface, and the adsorption of L-Met on the aluminum surface obeyed the Langmuir isotherm. The thermodynamic parameters (K_{ads} , ΔG°_{ads}) of adsorption for the studied inhibitor were calculated from their adsorption isotherm. The negative values of free energy of adsorption indicated that the adsorption of the inhibitor molecule is a spontaneous process.
- Surface morphological studied with Scanning Electron Microscopy (SEM) images showed that an inhibitor layer is formed on the electrode surface.

References:

- [1] R. Rosliza, W. B. W. Nik, *Current Applied Physics* 10 (2010) 221.
- [2] M. Abdulwahab, I.A. Madugu, S. A. Yaro, A. P. I. Popoola, *Silicon*, 4 (2) (2012) 137.
- [3] O. O. Ajayi, O. A. Omotosho, K. O. Ajanaku and B. O. Olawore, *Env. Res. J.* 5(4) (2011) 163.
- [4] M. Belkhaouda, L. Bazzi, R. Salghi, O. Jbara, A. Benlhachmi, B. Hammouti, J. Douglad, *J. Mater. Environ. Sci.* 1 (1) (2010) 25-33.
- [5] W. Carroll, M., Breslin, C. B. *J Br. Corros.* 26 (1991) 225.
- [6] A. El-Shafei, A. Abd El-Maksoud, S. A., Fouda, A. S. *Corros. Sci.* 46 (2004) 579.
- [7] F. Al-Karafi, M. Badawy, W. A. *Ind. J. Chem. Technol.* 3 (1996) 212.
- [8] M. Badawy, W. A., F. Al-Kharafi, M. El-Azab, A. A. *Corros. Sci.* 41 (1999) 709.
- [9] N. Sato, *Corros. Sci.* 37 (1995) 1947.
- [10] L. Garrigues, N. Pebere and F. Dabosi, *Electrochim. Acta*, 41 (1996) 1209
- [11] J. Diggle, W. Downie T.C. and C.W. Goulding, *Electrochim. Acta*, 15(7) (1970) 1079
- [12] M. Baumgaertner, and H. Kaesche, *Corros. Sci.*, 31 (1990) 231
- [13] DQ Zhang, LX Gao, GD Zhou. *CorrosSci.* 46(2004)3031.
- [14] M.A. Elmorsi, A.M. Hassanein. *CorrosSci.* 41(1999)2337.
- [15] H.O. Curkovic, E. Stupnisek-Lisac, H. Takenouti. *CorrosSci.* 52(2010) 398.
- [16] S.V. Lamaka, M.L. Zheludkevich, K.A. Yasakau, et al. *Electrochim Acta.* 52(2007) 7231.
- [17] V. Branzoi, F. Golgovici, F. Branzoi. *Mater Chem Phys.* 78(2003) 122.
- [18] M. Fleischmann, J.R. Hill, G. Mengoli, et al. *Electrochim Acta.* 30(1985) 879.
- [19] M. Sanja, M. Metikoš-Huković. *J Appl Electrochem.* 33(2003) 1137.
- [20] S.A. Umoren, I. B. Obot, E.E. Ebenso, P.C. Okafor, O. Ogbobe and E.E. Oguzi, *Anti.corros. Meth.Mater.* 73 (2006) 277-282.
- [21] T. suru, T. Haruyama, S. Gijutsu, B.J. *Jpn.Soc. Corros. Eng.* 27 (1978) 573.
- [22] J. Aljourani, K. Raeissi, M.A. Golozar, *Corros. Sci.* 51 (2009) 1836.

- [23] M. Messali, A. Bousskri, A. Anejjar, R. Salghi, B. Hammouti. *Int. J. Electrochem. Sci.*, 10 (2015) 4532 – 4551.
- [24] M. Kissi, M. Bouklah, B. Hammouti, M. Benkaddour, *Appl. Surf. Sci.*, 252(2006) 4190.
- [25] E. Machnikova, K.H. Whitmire, N. Hackerman, *Electrochim. Acta* 53(2008) 6024.
- [26] O. Olivares, N.V. Likhanova, B. Gomez, J. Navarrete, M.E. Llanos-Serrano, E. Arce, J.M. Hallen, *Appl. Surf. Sci.*, 252(2006) 2894.
- [27] F.M. Donahue, K. Nobe, *J. Electrochem. Soc.*, 112(1965) 886.
- [28] A. Stoyanova, G. Petkova, S.D. Peyrimhoff, *Chem. Phys.*, 279(2002), 1
- [29] E. Khamis, F. Bellucci, R.M. Latanision, E.S.H. El-Ashry, *Corros. Sci.*, 47(1991) 677.
- [30] O. Benali, L. Larabi, M. Traisnel, L. Gengenbre, Y. Harek, *Surf. Sci.* 253 (2007) 6130.
- [31] T. Szauer, A. Brandt, *Electrochim. Acta* 26(1981) 1253-1256
- [32] N. Guan, M.L. Xueming, L. Fei. *Chem. Phys.* 86 (2004) 59-68
- [33] E. Khamis, A. Hosney, S. El-Khodary, *Afinidad*, 52(1995) 95.
- [34] E. A. Noor, *Int. J. Electrochem. Sci.* 2 (2007) 996-1017.